Investigation of near source effects in array-based (SPAC) microtremor surveys

James Roberts and Michael Asten

Monash University

Abstract

Array-based methods for exploiting ambient seismic noise are receiving increasing attention in the literature, particularly for use in providing shear wave velocity profiles to assist with simulation of site-specific earthquake responses. Many of these microtremor methods - such as the spatial autocorrelation technique (SPAC) - operate under the fundamental assumption of plane wave propagation of surface waves. Although the SPAC technique has been successfully applied in urban areas, the effect of near-sources (and thus non-planar Rayleigh wave propagation) has received little attention. This paper explains the use of a simplified geometry-based modelling approach to compare near source effects for 4-station ("triangular") and 7-station ("hexagonal") arrays. Results of theoretical modelling and a field trial show that for near sources (3 array radii from array centre) with limited azimuthal range (1º source arc), the additional stations of the 7-station array mitigate near source effects whereas the SPAC spectrum for the 3-station array produces unreliable results.

Introduction

In recent times, the SPAC technique in particular has seen significant use in urban areas for a range of applications: (Apostolidis et al., 2004; Asten and Dhu, 2004; Asten et al., 2005; Bettig et al., 2001; Chavez-Garcia et al., 2005; Hartzell et al., 2005; Kudo et al., 2002; Roberts and Asten, 2004, 2005; Scherbaum et al., 2003; Wathelet et al., 2005). It is the relatively high level of (high frequency) microtremor energy present in urban areas that makes towns and cities attractive locations for microtremor surveys. In most of the literature, the sources contributing to the microtremor 'wave-field' are considered to be located at significant distance from the array, allowing for the assumption of plane-wave surface wave propagation. Near source effects in microtremor work have received little attention.

The consequences for microtremor measurements resulting from receivers being located close to the microtremor sources can potentially include three distinct effects: non-planar wavefront geometry, dominance of body wave energy rather than surface wave energy, and an increased likelihood for the presence of higher modes in the wave field. The latter two aspects are addressed in many studies associated with the (active) SASW and MASW techniques, eg. Xia et al., 2004, and are not addressed in this paper.

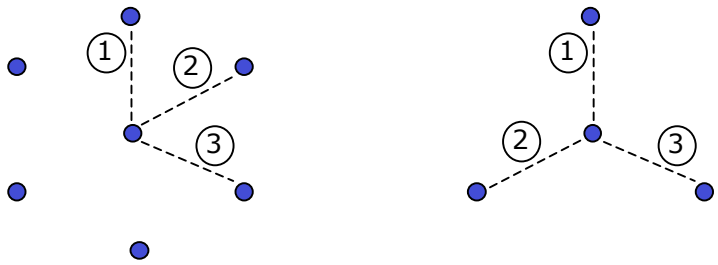

Figure 1: 7-station and 4-station array geometry. Although the 7-station array allows for better statistical averaging of ground motion, it samples only the same azimuths (defined by alignment of station pairs as indicated by the dashed lines) as an equivalent 4-station array.

Recent research by Okada (2006) compared the efficiency of 4-station (triangular) and 7-station (hexagonal) array geometries (Figure 1) for the far-field case. Professor Okada's results showed that the additional stations in the 7-station array configuration did not result in any analytical advantage in minimizing errors associated with only sampling a finite number of azimuths. This paper compares the performance of 4- and 7-station array geometry at a range of source distances.

Geometric modelling of SPAC spectra

The modelling approach adopted here is an extension of that used by Asten (2003; 2006) and Asten et al. (2004) for assessing the performance of differing array geometries in situations where microtremor sources are confined to a fixed range of azimuths. This approach uses a numerical summation of sources, with a single "source" for each 1º of source arc to be analyzed. Thus, continuous source arcs consisting of 1 to 360 sources can be placed in arbitrary positions around the array. For the near source modelling presented here, a further variable is added to the method described by Asten (2003), allowing the sources to be placed at a (finite) fixed distance from the array. This distance is defined in units of array radii (r) measured from the array centre.

The coherency ($\rho_{a,b}$) for a single pair of sensors (a and b) in the presence of an arc of identical sources producing monochromatic waves of wavenumber (k) could be calculated by a simple summation of the differences in phase of each source at each of the sensor positions:

$$\rho_{a,b} = \frac{1}{w_{total}} \sum_{j=1}^{n} w_{f(aj)} w_{f(bj)} e^{i\left(\phi_{a,j} - \phi_{b,j}\right)} \qquad (1)$$

where: ρ is the coherency, ϕ is the phase of waves from each source (j) at each geophone pair, n is the total number of sources, w_f is the weighting factor for each sensor based on distance from the source and w_{total} is the sum of all the weighting factors used inside the summation.

For the far-field case, all sources were considered to contribute equally to the model coherency for a given array configuration (Asten, 2003). Due to the effects of attenuation, for extremely near sources the signal coherency could be biased towards sources that are closer than others. To account for this, weighting factors based on the relative distance of each sensor to the source is added into the summation process (see equation (1)). By repeated application of equation (1), the average model SPAC spectrum ($\overline{\rho}$) for an entire array of sensors can then be calculated by an average of $\rho_{a,b}$ for all of the station pairs in the array.

For surface waves, geometric attenuation of wave energy follows a 1/r relationship with distance from the source, although this rate is for stable far-field propagation. Attenuation of wave energy associated with inelastic losses or absorption is at a rate dependant on frequency and the material properties (specifically the quality factor, Q) of the medium. The weighting factors in equation (1) are calculated using a geometric decay parameter (α) applied to the relative source distance for the station pairs. A value of α=1.0 corresponds to purely geometric decay, with higher values indicating additional attenuation associated with absorption and scattering. A more detailed description of the modelling procedure is given in Roberts and Asten (2006).

Modelling examples

To compare the performance of the 4-station and 7-station array configurations for varying source distances, model SPAC spectra were computed for a range of source distributions, for (dimensionless) source distances of 99r, 6r, 3r and 1.5r, where r corresponds to the array radius. For broad source distributions consisting of more than 90º of sources, the performance of the two array configurations was similar, consistent with the findings of Okada (2006). However, a significant difference is seen for narrow

azimuthal distributions of sources under near-source conditions. This is best illustrated for the case of a single (1º) source located as shown in Figure 2. Each plot in the figure compares the model SPAC curve (heavy solid line) compared with the ideal result expected for a halfspace with full (360º) azimuthal coverage – a Bessel function (J_0) shown as a thin solid line. The dashed line is the imaginary component, which is not discussed here.

Comparison of the spectra for the 4-station (triangle) and 7-station (hexagon) arrays at each source distance in Figure 2 reveals a large difference in the performance of the two arrays for a single near source. In the far field case (99r), both arrays yield identical results. In fact, the plot for the 4-station array, far field (99r) case here (Figure 2) is identical (save for use of a linear k.r axis) to that of Figure 1(c) in Okada (2006).

For a source placed at a distance of 6.0r from the array centre (at an azimuth co-linear with a sensor pair) the 7-station array model displays little difference in the real coherency component to the far field case for values of kr up to the first minimum of the J_0 curve (which is the part of the curve most critical to interpretation and inversion of SPAC spectra). In fact, even at source distances of 3.0r and 1.5r, no large deviations from the J_0 'ideal' are observed below approximately kr ≈3. In contrast to the relatively small near source effects for the 7-station (hexagonal) array, the near-source model spectra for the 4-station (triangular) array displays significant deviations from J_0 at kr < 3, beginning with a source distance as large as 6.0r. For the source distances of 3.0 and 1.5r, the deviation from J_0 is very large and extends to kr values as low as 1.

The implications for this difference in behaviour for the 4- and 7-station arrays in the presence of a single (omnidirectional) near-source are two-fold: First, the portion of the coherency curve up to k.r ≈3 can, in principle, be used to produce dispersion curves when only a single near-field source is present provided the geometry of the source is co-linear with any of the sensor pairs in a 7-station array. Second, the performance (and efficiency as described by Okada (2006)) of the relatively sparse 4-station (triangular) array is much more susceptible to near-source effects than a 7-station (hexagonal) array placed with similar source-sensor geometry.

Field validation of array comparison

In order to evaluate the validity of the theoretical near-source effects predicted from the modelling, a field trial was designed with the intention of reproducing some of the model source conditions of Figure 2. A rural location, away from any urban areas, was chosen to minimise the background level of high-frequency microtremor energy. The chosen site was at Laanecoorie, in Victoria Australia, which is known from previous investigations to have predominately horizontal stratigraphy consisting of alluvial sand and clay deposits.

A 10m radius hexagonal array consisting of seven Mark Products L28 seismometers (natural frequency ~5.5 Hz) was used to record a series of 300-second duration files of ground motion. The time domain data were processed using methodology identical to that described by Roberts and Asten (2004; 2005) to produce MMSPAC (Asten et al., 2004) spectra for differing station separations in the hexagonal array. The hexagonal configuration also allows for the processing of the data for two sub-triangles (4-station arrays) to enable comparison of these different array configurations.

For the 10m radius array, files of 300 seconds duration were recorded in the presence of a standard four wheel drive vehicle driving continuously along a circular path at distances of 15m, 20m, 30m and 40m from the array centre. The source path and distances were chosen to mimic the source distribution available in the modelling procedure corresponding to source distances of 1.5r, 2.0r, 3.0r and 4.0r and 360º of azimuthal distribution.

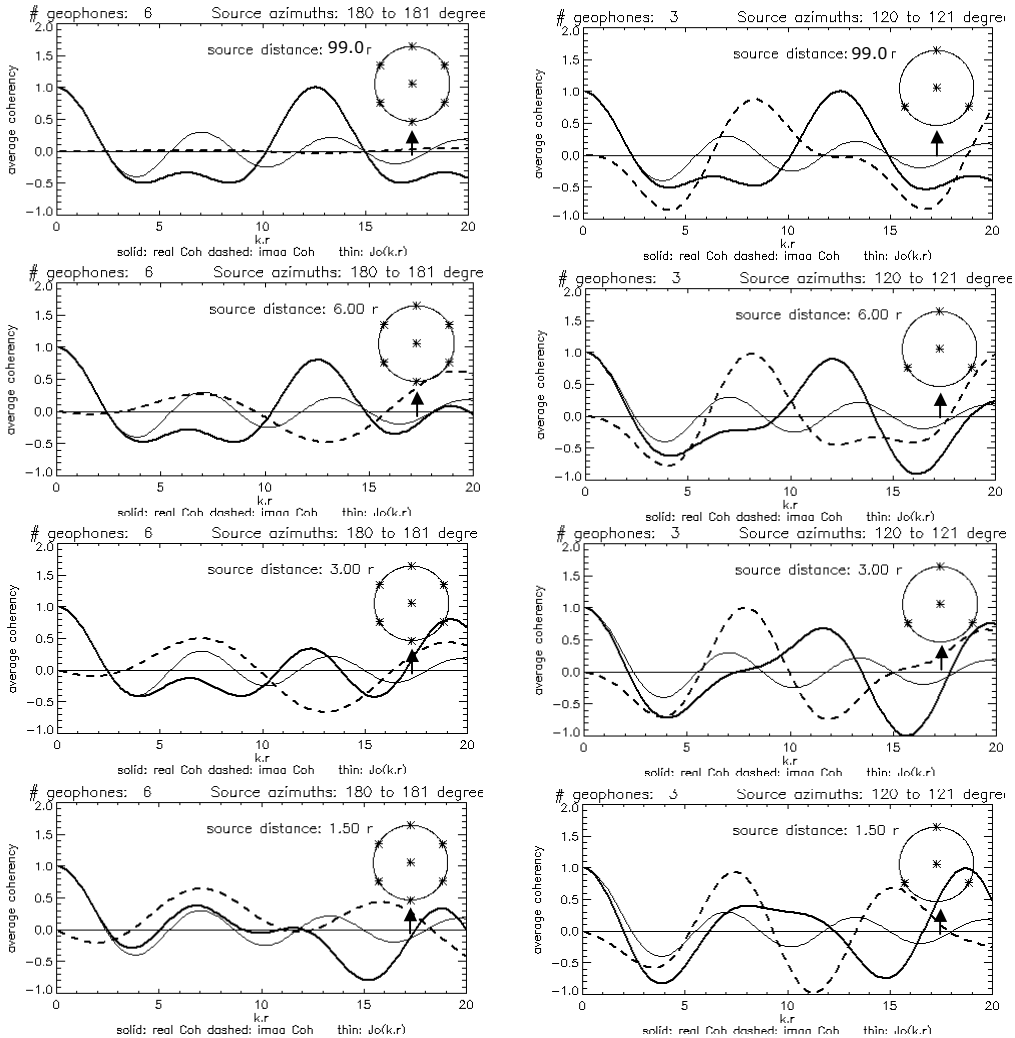

Figure 2: Model SPAC spectra (heavy lines represent the real component; dashed lines represent the imaginary component) compared to J_0 curves (thin lines) for source distances of (top to bottom) 99r, 6.0r, 3.0r and 1. 5r. Models on the left use a 7-station (hexagonal) array; models on the right use a 4-station (triangular) array. All models are the result of 1º of microtremor sources (direction shown by arrow), a geometric decay index (α) of 1.0 and display the average for radial pairs of sensors.

Several files were recorded simulating a 'point' source of microtremor energy (simulated by driving a vehicle backwards and forwards along a radial path outside the array) in various positions relative to the orientation of sensor pairs. Figure 3 shows the SPAC spectrum resulting from a 'point' source located in-line with one of the sensor pairs in a 7-station array (the whole hexagon), along with the two sub arrays consisting of 4-station triangles, each offset 60º in azimuth from the other.

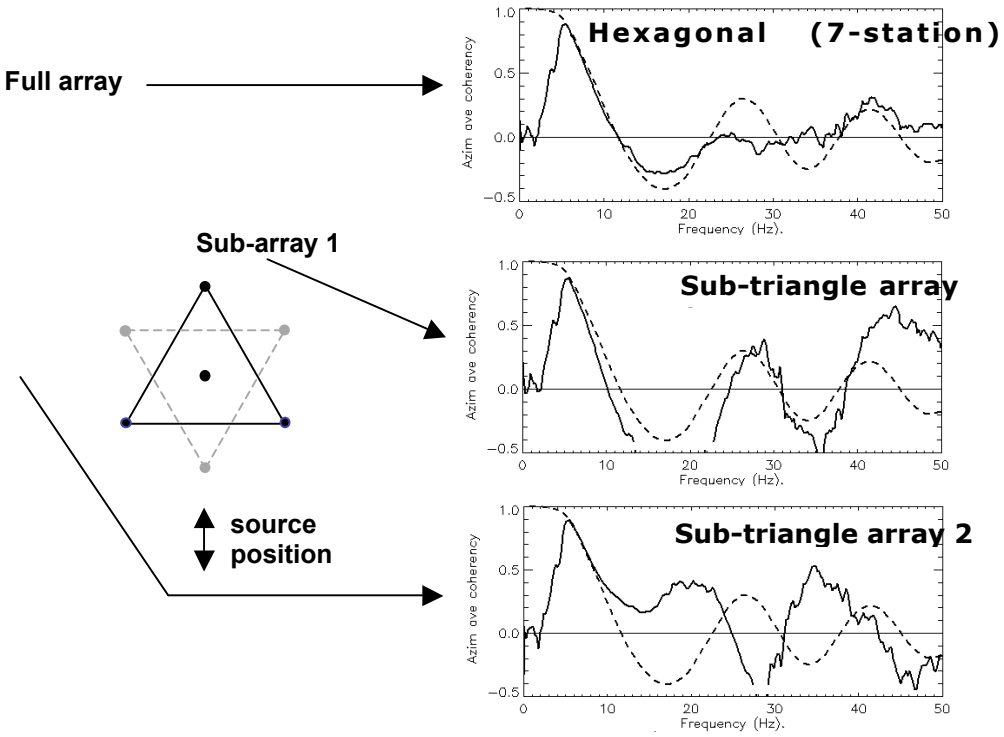

Figure 3: Results for 'point' source located in-line with a sensor pair. Radial averages for the full array (hexagon) and two 4-station (triangular) sub-arrays. Source distance is approximately 30m (3.0r). Thick line is field SPAC; dashed line is reference model SPAC obtained using a 360º source distribution for the 7-station array (same in all three plots).

The plot for the hexagonal array shows that the SPAC curve still fits (up to approximately 25 Hz) the reference model (dashed line) obtained from a 360º distribution of distant (4.0r) sources. However, the two sub-arrays consisting of conjugate 4-station triangles show very large departures from the reference model at all frequencies above approximately 7 Hz. The deviation from the reference model for sub-triangle array 1 is very similar (especially below 25 Hz) to those predicted by the modelling for the triangular arrays in Figure 2.

From these results we can infer that even though Okada (2006) demonstrated the equivalent efficiency for 7-station and 4-station arrays for far-field sources, the 7-station configuration allows for better performance of the array in the presence of near-sources.

Conclusions

Although the modelling procedure presented here makes a number of simplifying assumptions and the source distributions used are highly contrived, the results are useful in providing some indication as to the influence of source distance on the nature of observed SPAC spectra using 7-station and 4-station arrays.

Although 7-station (hexagonal) and 4-station (triangular) arrays sample an identical number of azimuths, the additional stations in the 7-station array make this configuration more reliable under near source conditions. Under near source conditions, the use of the sparser 4-station configuration may lead to significant distortions in the observed SPAC spectra.

This study has also shown that it is possible in both theory and practice to obtain SPAC curves that are reliable up to the first spectral minimum using a single source and a 7-station (hexagonal) array. The reader is directed to Roberts and Asten (2006) for additional results of the near source modelling outlined in this paper.

References

Apostolidis, P., Raptakis, D., Roumelioti, Z. and Pitilakis, K. (2004). Determination of S-wave velocity structure using microtremors and spac method applied in Thessaloniki (Greece). Soil Dynamics and Earthquake engineering 24 (1), 49-67.

Asten, M.W. (2003). Lessons from alternative array design used for high-frequency microtremor array studies: Earthquake Risk Mitigation - Proceedings of the Annual Conference of the Australian Earthquake Engineering Society, Paper 14. AEES Conference, Melbourne, Australia, 27-28 November, 2003.

Asten, M.W. (2006). On bias and noise in passive seismic data from finite circular array data processed using SPAC methods. Geophysics [in press].

Asten, M.W. and Dhu, T. (2004). Site response in the Botany area, Sydney, using microtremor array methods and equivalent linear site response modelling. Australian Earthquake Engineering in the New Millenium - where to from here? Proceedings of the annual conference of the Australian Earthquake Engineering Society, Paper 33. AEES Conference, Mt. Gambier, Australia, 5-7 November, 2004.

Asten, M.W., Dhu, T. and Lam, N. (2004). Optimised array design for microtremor array studies applied to site classification; comparison of results with SCPT logs. 13th Wold Conference on Earthquake Engineering, Paper No. 2903.

Asten, M.W., Stephenson, W.R. and Davenport, P.N. (2005). Shear-wave velocity profile for Holocene sediments measured from microtremor array studies, SCPT, and seismic refraction. Journal of Environmental and Engineering Geophysics 10 (3), 235-242.

Bettig, B., Bard, P.Y., Scherbaum, F., Riepl, J., Cotton, F., Cornou, C. and Hatzfeld, D. (2001). Analysis of dense array noise measurements using the modified spatial auto-correlation method (SPAC): application to the Grenoble area. Bollettino di Geofisica Teorica ed Applicata 42, 281-304.

Chavez-Garcia, F.J., Rodriguez, M. and Stephenson, W.R. (2005). An alternative approach to the SPAC analysis of microtremors: exploiting the stationarity of noise: Bulletin of the Seismological Society of America 95 (1), 277-293.

Hartzell, S., Carver, D., Seiji, T. and Herrmann, R. (2005). Shallow shear-wave velocity measurements in the Santa Clara Valley; comparison of SPAC and FK methods. [extract from] USGS Open File Report 2005-1169.

Kudo, K., Kanno, T., Okada, H., Ozel, O., Erdik, M., Sasatani, T., Higashi, S., Takahashi, M. and Yoshida, K. (2002). Site-specific issues for strong ground motions during the Kocaeli, Turkey, earthquake of 17 August 1999, as inferred from array observations of microtremors and aftershocks. Bulletin of the Seismological Society of America 92 (1), 448-465.

Okada, H. (2006). Theory of efficient array observations of microtremors with special reference to the SPAC method. Exploration Geophysics 37 (1), 73-84.

Roberts, J. and Asten, M. (2004). Resolving a velocity inversion at the geotechnical scale using the microtremor (passive seismic) survey method. Exploration Geophysics 35 (1), 14-18.

Roberts, J. and Asten, M. (2005). Estimating the shear velocity of Quaternary silts using microtremor array (SPAC) measurements. Exploration Geophysics 36 (1), 34-40.

Roberts, J. and Asten, M. (2006). Investigation of near source effects in array-based (SPAC) microtremor surveys. Proceedings of the 3rd International Symposium on the Effects of Surface Geology on Seismic Motion (ESG2006). Vol 1. Grenoble, France, 30 August – 1 September 2006.

Scherbaum, F., Hinzen, K.G. and Ohrnberger, M. (2003). Determination of shallow shear wave velocity profiles in the Cologn, Germany area using ambient vibrations. Geophysical Journal International 152, 597-612.

Wathelet, M., Jongmans, D. and Ohrnberger, M. (2005). Direct inversion of spatial autocorrelation curves with the neighborhood algorithm. Bulletin of the Seismological Society of America 95 (5), 1787-1800.

Xia, J., Miller, R.D., Park, C.B., Ivanov, J.I., Tian, G. and Chen, C. (2004). Utilization of high-frequency Rayleigh waves in near-surface geophysics. The Leading Edge 23 (8), 753-759.